environmental microbiology

Environmental Microbiology (2022) **24**(3), 1308–1325 doi:10.1111/1462-2920.15824

Prevalence, complete genome, and metabolic potentials of a phylogenetically novel cyanobacterial symbiont in the coral-killing sponge, *Terpios hoshinota*

Yu-Hsiang Chen,[1,2,3†] **Hsing-Ju Chen**,[3†] **Cheng-Yu Yang**,[3] **Jia-Ho Shiu**,[3] **Daphne Z. Hoh**,[3,4,5] **Pei-Wen Chiang**,[3] **Wenhua Savanna Chow**,[3,4,5] **Chaolun Allen Chen**,[3,4] **Tin-Han Shih**,[3] **Szu-Hsien Lin**,[3] **Chi-Ming Yang**,[3] **James Davis Reimer**,[6,7] **Euichi Hirose**,[6] **Budhi Hascaryo Iskandar**,[8] **Hui Huang**,[9] **Peter J. Schupp**,[10] **Chun Hong James Tan**,[11,12] **Hideyuki Yamashiro**,[7] **Ming-Hui Liao**[3] and **Sen-Lin Tang**[2,3,4,5*]

[1]*Bioinformatics Program, Taiwan International Graduate Program, National Taiwan University, Taipei, Taiwan.*

[2]*Bioinformatics Program, Institute of Information Science, Taiwan International Graduate Program, Academia Sinica, Taipei, Taiwan.*

[3]*Biodiversity Research Center, Academia Sinica, Taipei, Taiwan.*

[4]*Biodiversity Program, Taiwan International Graduate Program, Academia Sinica and National Taiwan Normal University, Taipei, Taiwan.*

[5]*Department of Life Science, National Taiwan Normal University, Taipei, Taiwan.*

[6]*Department of Chemistry, Biology and Marine Science, Faculty of Science, University of the Ryukyus, Nishihara, Okinawa, Japan.*

[7]*Tropical Biosphere Research Center, University of the Ryukyus, Nishihara, Okinawa, Japan.*

[8]*Department of Fishery Resources Utilization, Faculty of Fisheries and Marine Science, Bogor Agricultural University, Bogor, Indonesia.*

[9]*Tropical Marine Biological Research Station in Hainan, Chinese Academy of Sciences, Sanya, China.*

[10]*Institute of Chemistry and Biology of the Marine Environment, University of Oldenburg, Wilhelmshaven, Germany.*

[11]*Faculty of Science and Marine Environment, Universiti Malaysia Terengganu, Kuala Nerus, Terengganu, Malaysia.*

[12]*Institute of Oceanography and Environment, Universiti Malaysia Terengganu, Kuala Nerus, Terengganu, Malaysia.*

Received 17 May, 2021; accepted 13 October, 2021. *For correspondence. E-mail sltang@gate.sinica.edu.tw; Tel. (+886) 2 27893863; Fax (+886) 2 27890844. †These authors contributed equally to this work.

Summary

Terpios hoshinota **is an aggressive, space-competing sponge that kills various stony corals. Outbreaks of this species have led to intense damage to coral reefs in many locations. Here, the first large-scale 16S rRNA gene survey across three oceans revealed that bacteria related to the taxa *Prochloron*, *Endozoicomonas*, SAR116, *Ruegeria*, and unclassified *Proteobacteria* were prevalent in *T. hoshinota*. A *Prochloron*-related bacterium was the most dominant and prevalent cyanobacterium in *T. hoshinota*. The complete genome of this uncultivated cyanobacterium and pigment analysis demonstrated that it has phycobiliproteins and lacks chlorophyll *b*, which is inconsistent with the definition of *Prochloron*. Furthermore, the cyanobacterium was phylogenetically distinct from *Prochloron*, strongly suggesting that it should be a sister taxon to *Prochloron*. Therefore, we proposed this symbiotic cyanobacterium as a novel species under the new genus *Candidatus* Paraprochloron terpiosi. Comparative genomic analyses revealed that 'Paraprochloron' and *Prochloron* exhibit distinct genomic features and DNA replication machinery. We also characterized the metabolic potentials of 'Paraprochloron terpiosi' in carbon and nitrogen cycling and propose a model for interactions between it and *T. hoshinota*. This study builds a foundation for the study of the *T. hoshinota* microbiome and paves the way for better understanding of ecosystems involving this coral-killing sponge.**

Introduction

The coral-killing sponge *Terpios hoshinota* has received attention since outbreaks were first detected in several coral reef regions in the western Pacific Ocean, South China Sea, and Indian Ocean (Rützler and Muzik, 1993; Liao *et al*., 2007; Fujii *et al*., 2011; de Voogd *et al*., 2013;

Hoeksema *et al*., 2014; Montano *et al*., 2015; Thinesh *et al*., 2015). This sponge grows up to 23 mm $^{-1}$ month^{-1} (Plucerrosario, 1987), and its fast-growing and competitive nature enables it to kill scleractinian corals rapidly and at a high rate (30%–80% mortality) across biogeographic regions (de Voogd *et al*., 2013; Hoeksema *et al*., 2014; Montano *et al*., 2015; Yomogida *et al*., 2017). For instance, *T. hoshinota* overgrowth jeopardizes coral reefs in numerous regions of Taiwan, Indonesia, Malaysia, Japan, India, and the Great Barrier Reef (Fujii *et al*., 2011; Shi *et al*., 2012; Madduppa *et al*., 2017; Yomogida *et al*., 2017). The gradual spread of *T. hoshinota* poses a serious threat to coral reefs. However, little is known regarding the causes of such outbreaks.

Sponges are commonly known to harbour complex microbial communities, and symbiotic microorganisms play vital roles in the development, health, and nutrient acquisition of their hosts (Hentschel *et al*., 2012). The microbes and hosts form an ecological unit referred to as a holobiont. In *T. hoshinota*, the sponge is associated with a bacterial community of relatively low diversity that is dominated by cyanobacteria (Tang *et al*., 2011). Ultrastructural observations have clearly shown that cyanobacteria are densely distributed in *T. hoshinota*, contributing to 50% of the total cellular volume (Rützler and Muzik, 1993; Hirose and Murakami, 2011; Tang *et al*., 2011), and the blackish colour of *T. hoshinota* has been attributed to cyanobacteria (Tang *et al*., 2011). Accordingly, the sponge has been called 'cyanobacteriosponge' (Rützler and Muzik, 1993). Several studies have shown that cyanobacteria play important roles in the growth of *T. hoshinota* and in competition with corals. For instance, a high number of cyanobacteria can be observed in the larvae of *T. hoshinota* (Wang *et al*., 2012a; Hsu *et al*., 2013), suggesting that they are transmitted vertically during embryogenesis in this particular sponge (Nozawa *et al*., 2016). Second, *in situ* short-term shading can cause a long-term decrease in the biomass of symbiotic cyanobacteria and lead to irreversible damage to *T. hoshinota*, arresting its expansion (Soong *et al*., 2009; Thinesh *et al*., 2017). Third, when *T. hoshinota* encounters certain corals, the sponge forms a hairy tip structure packed with dense cyanobacteria to interact with corals (Wang *et al*., 2012b). These results indicate that *T. hoshinota*-associated cyanobacteria are vital for the overgrowth and rapid destruction of coral reef ecosystems.

Although important, the identity and classification of dominant symbiotic cyanobacteria in *T. hoshinota* are still unclear. In 2015, Yu *et al*. isolated and cultivated *Myxosarcina* sp. GI1, a baeocytous cyanobacterium, from *T. hoshinota* at Green Island (Yu *et al*., 2015). However, electron microscopy did not identify vegetative cell aggregates of baeocytes, a type of reproductive cell, in *T. hoshinota* (Hirose and Murakami, 2011; Tang *et al*., 2011; Wang *et al*., 2012a). Moreover, our previous analyses of 16S rRNA gene sequences in *T. hoshinota* samples from Green Island revealed that the dominant cyanobacterium in *T. hoshinota* is closely related to *Prochloron* (Tang *et al*., 2011). *Prochloron*, a genus comprised of a single species, is an obligate symbiont of certain ascidians; the hallmarks and definition of this genus are the presence of chlorophyll *a* and *b* and the lack of phycobilins, which are unusual in cyanobacteria (Whatley, 1977). However, pigment analysis identified that the cyanobacteria in *T. hoshinota* contain phycobilins (Hirose and Murakami, 2011). Hence, the characteristics and classification of the predominant cyanobacterium in *T. hoshinota* remain uncertain. Moreover, whether the predominant cyanobacterium is the same in all of the Indo-Pacific regions requires validation. Finally, since cyanobacteria are attributed to the health and invasive capacity of *T. hoshinota*, ecological relationships and molecular interactions involving *T. hoshinota* and its cyanobacteria need to be determined.

Other *T. hoshinota*-associated bacteria may also contribute to holobiont function. The microbial community in a sponge can be shaped by host-related factors, such as the immune system and nutrient exchange (Pita *et al*., 2013; Webster and Thomas, 2016; Pita *et al*., 2018), or be determined by environmental factors, such as light availability, pH, and temperature (Webster and Thomas, 2016). Nevertheless, no study has investigated the microbiome of *T. hoshinota* from different biogeographical backgrounds. Hence, in this study, we conducted a 16S ribosomal RNA (rRNA) gene survey to investigate the microbial community structures and diversity of *T. hoshinota* samples from a wide geographical range across the western Pacific Ocean, South China Sea, and Indian Ocean. Knowing that the predominance of a cyanobacterium was ubiquitous, the complete genome of this uncultivated cyanobacterium was reconstructed by whole-genome shotgun sequencing using Nanopore and Illumina platforms. Genomic and comparative genomic analyses elucidated the phylogenetic affiliation and taxonomy of the dominant symbiotic bacterium in *T. hoshinota* and identified putative symbiotic interactions between the bacterium and the host.

Results

Bacterial diversity and community in T. hoshinota *were geographically dependent*

16S rRNA gene sequencing was performed on *T. hoshinota* samples collected from 15 locations across three oceans (Supporting Information Table S1). To evaluate the effects of sampling sites on alpha and beta diversity, sites with sample numbers >2 were used to

perform statistical tests. Samples collected from different sites had distinct amplicon sequence variant (ASV) richness and diversity (Supporting Information Fig. S1). A statistical test showed that ASV richness estimated by Chao1 was significantly different across sampling sites (Kruskal–Wallis: $P = 0.007$). ASV diversity indices, including Shannon and Faith's phylogenetic diversity (PD), were also significantly associated with sampling sites (Kruskal–Wallis: $P = 0.0002$ for Shannon index, and $P = 0.007$ for PD index). To exclude any effects of collection year on diversity indices, we compared the diversity indices of the samples from JPBS, TWLD, and TWLY collected in 2010. Kruskal–Wallis tests showed that the diversity indices, except for the PD index, were different across samples from the three sites (Chao1: $P = 0.043$, Shannon: $P = 0.022$, and PD index: $P = 0.068$).

Samples from different locations shared distinct microbial community structures based on Bray–Curtis distance matrix [permutational analysis of variance (PERMANOVA): pseudo-$F = 7.2287$, $P = 0.004$] (Fig. 1A). When phylogenetic relatedness of the ASVs was incorporated into beta diversity analysis by unweighted UniFrac, the differences were still statistically significant (pseudo-$F = 2.238$, $P = 0.029$) (Fig. 1B). Moreover, when abundance information was taken into consideration for UniFrac, the effect of the sampling sites on dissimilarities increased according to pseudo-F values (weighted UniFrac: pseudo-$F = 8.2522$, $P = 0.02$) (Fig. 1C). Twenty one of 28 pairwise comparisons for weighted UniFrac and Bray–Curtis distances of bacterial communities using PERMANOVA showed significant differences ($P < 0.05$). However, the bacterial communities in samples collected from TWLD, TWLY, and TWKT, which are located in southern Taiwan, were not significantly different from each other.

Prochloron-*related bacterium dominated* T. hoshinota *microbial communities across different oceans*

From 61 samples, we recovered 3256 ASVs in total. *Cyanobacteria* and *Proteobacteria* were predominant and prevalent. They accounted for 84.1%–97.9% relative read abundance and were present in all samples (Fig. 2 and Fig. S2A). Besides the two phyla, *Bacteroidetes*- and *Spirochaetae*-related ASVs were also present across all of the samples, although their relative read abundances were only 0.77%–9.61%. At the genus level, we found that genera related to *Prochloron*, SAR116_clade, and *Ruegeria* were present in all samples, and their mean relative read abundance was 30%, 14%, and 2.7%, respectively (Supporting Information Fig. S2B). In addition to these generic-level groups, *Endozoicomonas* was present in 90% of samples, and the mean relative read abundance was 8.1%.

Of the 3256 ASVs, four were present in at least 90% of the samples, forming a core microbiome (Table 1), which accounted for an average of 50% of the relative read abundance (Table 1). Among them, ASV#1, annotated as *Prochloron*, was dominant and was present in all samples. This ASV, referred to as ASV1-Prochloron, made up 30% of the relative read abundance, on average. In addition, ASV1-Prochloron accounted for most of the relative abundance of *Cyanobacteria* in the samples (Supporting Information Table S2). Other members of the core microbiome included ASVs that were related to *Proteobacteria* (ASV#2, mean relative abundance = 1.9%), *Rhodobacteraceae* (ASV#3, mean relative abundance = 7.6%), and *Pseudospirillum* (ASV#4, mean relative abundance = 9.6%). These ASVs shared low identities with their best matches in NCBI using BLASTn, indicating that the bacteria were novel (Table 1).

Structure of symbiotic Prochloron-*related bacteria in* T. hoshinota

To reveal the clear and detailed structure of *T. hoshinota* and its *Prochloron*-related bacteria, a rubber tire was attached underwater in front of a *T. hoshinota* with epoxy putty. After the *T. hoshinota* had encrusted the tire, the sample was collected and observed under a scanning electron microscope (SEM). (Fig. 3). The *T. hoshinota* sponge, approximately 500 μm in diameter, was supported by bundles of tylostyle spicules interlaced on the surface (Fig. 3A and B). Inside the body, spherical bacterial cells of 4–6 μm diameter were widely distributed, and cells were observed at various stages of cell division (Fig. 3C and F). No vegetative cell aggregates of baeocytes were observed from our results, indicating that *Myxosarcina* sp. was not the dominant cyanobacterium. Transmission electron microscopy (TEM) results showed that these spherical cells contained thylakoids, which are typical compartments inside cyanobacteria, and their arrangements were parietal (Fig. 3D–F). In addition, carboxysomes were identified, and gas vesicles were absent from these cells.

Genome assembly of a novel Prochloron-*related species*

The predominance of a *Prochloron*-related ASV in *T. hoshinota* from various locations indicated an intimate association between the bacterium and *T. hoshinota*. To reveal the identity and characteristics of the *Prochloron*-related bacterium, a genome, referred to as LD05, was reconstructed by *de novo* assembly of the metagenome assembled from a sample collected at Green Island, Taiwan (Fig. 4). Using a combination of Illumina and Nanopore sequencing, we successfully recovered a single circular contig, which was annotated as a

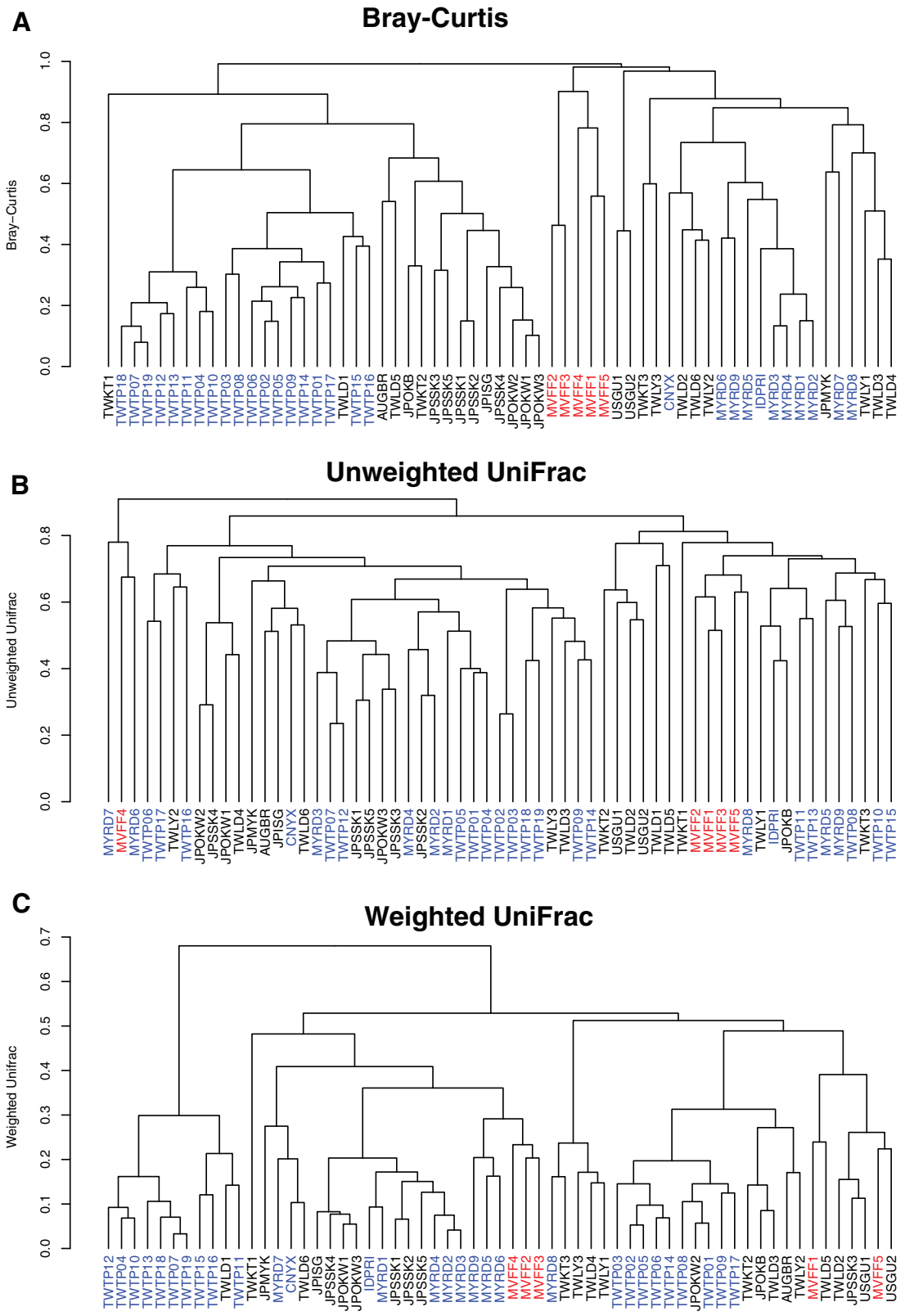

Fig 1. Dendrograms of beta diversity analysis.
Dendrograms of beta diversity analysis using the Bray–Curtis metric (A), unweighted (qualitative) UniFrac (B), and weighted (quantitative) UniFrac (C). Samples collected from western Pacific Ocean, Indian Ocean, and South China Sea are coloured with black, red, and blue, respectively.

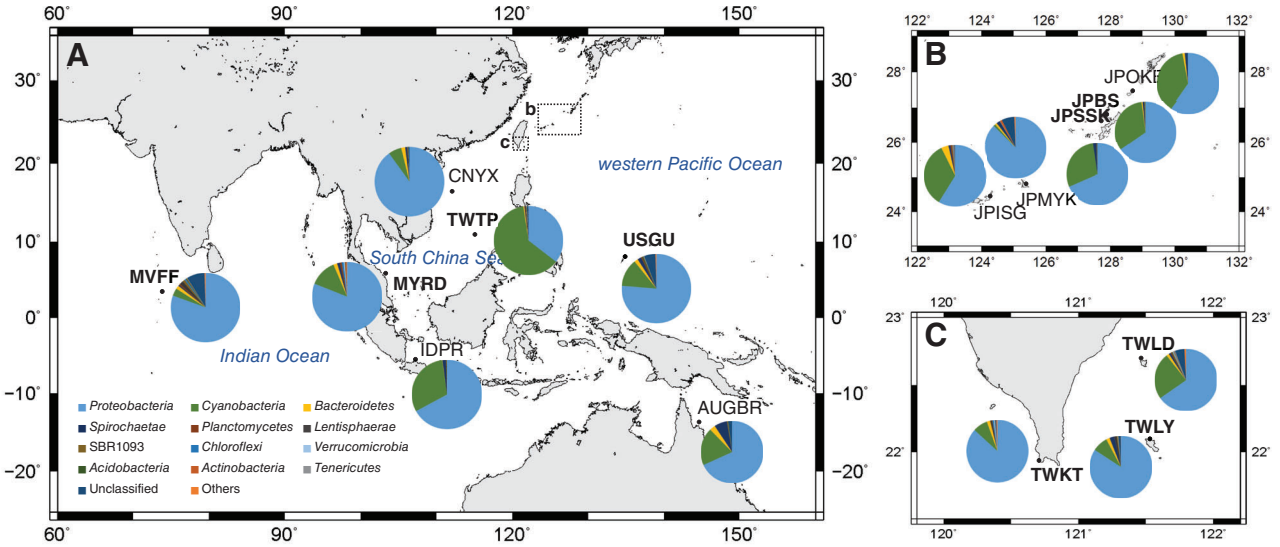

Fig 2. Proportions of *T. hoshinota*-associated bacterial communities across oceans.
Proteobacteria (blue) and *Cyanobacteria* (green) were the dominant groups, ranging from 84.1% to 97.9% of each community.
A. Bacterial compositions across the western Pacific Ocean, South China Sea, and Indian Ocean. Maps on the right show results in Okinawa, Japan (B), and Taiwan (C). Different colours represent different bacterial phyla. Percentage composition of phyla less than 0.05% are grouped as 'Others'.

Table 1. Core bacterial members in *T. terpios* and their best matches in NCBI.

ASV_ID	Classification by mothur	Median relative abundance (%)	Mean relative abundance (%)	% of sample (%)	Best hit in NCBI	Identity (%)
ASV#1	*Prochloron*	29.6	30.9	100	*Synechocystis* sp. PLV1 (JX099359.1)	97.52
ASV#2	unclassified *Proteobacteria*	1.3	1.9	100	*Pseudomonas parafulva* (MN203982.1)	92.68
ASV#3	unclassified *Rhodobacteraceae* (α-*Proteobacteria*)	6.5	7.6	97	*Marimonas arenosa* (MW828566.1)	95.85
ASV#4	*Pseudospirillum* (γ-*Proteobacteria*)	6.0	9.6	93	γ-*proteobacterium* EHK-1 (AF228694.1)	88.18

cyanobacterium without any sequence gaps. The mapping coverage of Illumina reads was 99.98% of the metagenome-assembled genome (MAG), and the mean depth was 983-fold.

The complete MAG, which was 3.8 Mbp, contained two copies of 16S and 23S rRNA gene sequences (Fig. 4 and Table 2) and 46 tRNA genes; one of the 16S rRNA gene sequences was 100% identical to that of the predominant ASV1-Prochloron identified from the 16S rRNA gene survey. Analysis of the GTDB-Tk demonstrated that the LD05 MAG was closest to *Prochloron didemni*, but with only 77.97% average nucleotide identity (ANI).

Recently, a putative *Prochloron* species genome termed SP5CPC1 was recovered from the metagenome of a sponge microbiome (Podell *et al*., 2020). ANI analysis identified that the LD05 genome shares 93.18% identity with the SP5CPC1 genome, which is below the 95% ANI cutoff for species delineation (Richter and Rossello-Mora, 2009). LD05 shares a similar genome size, GC ratio, and coding density as SP5CPC1 (Supporting Information Table S3). In contrast, *P. didemni* P2-P4 had a much larger genome, a lower GC ratio, and lower coding densities (Supporting Information Table S3). There was also a discrepancy between LD05 and *P. didemni* P2-P4 based on the average amino acid identity (AAI) and percentage of conserved proteins (POCPs) analyses (Supporting Information Fig. S3). LD05 shared 91% AAI with SP5CPC1, but only 70% AAI with *P. didemni* P2–P4 genomes. On the other hand, the POCP between LD05 and *Prochloron* genomes ranged from 49.8% to 52%, close to a proposed 50% POCP cutoff for genera delineation (Qin *et al*., 2014). Taken together, the LD05 and SP5CPC1 genomes were of different species, and both were more distantly related to *P. didemni*.

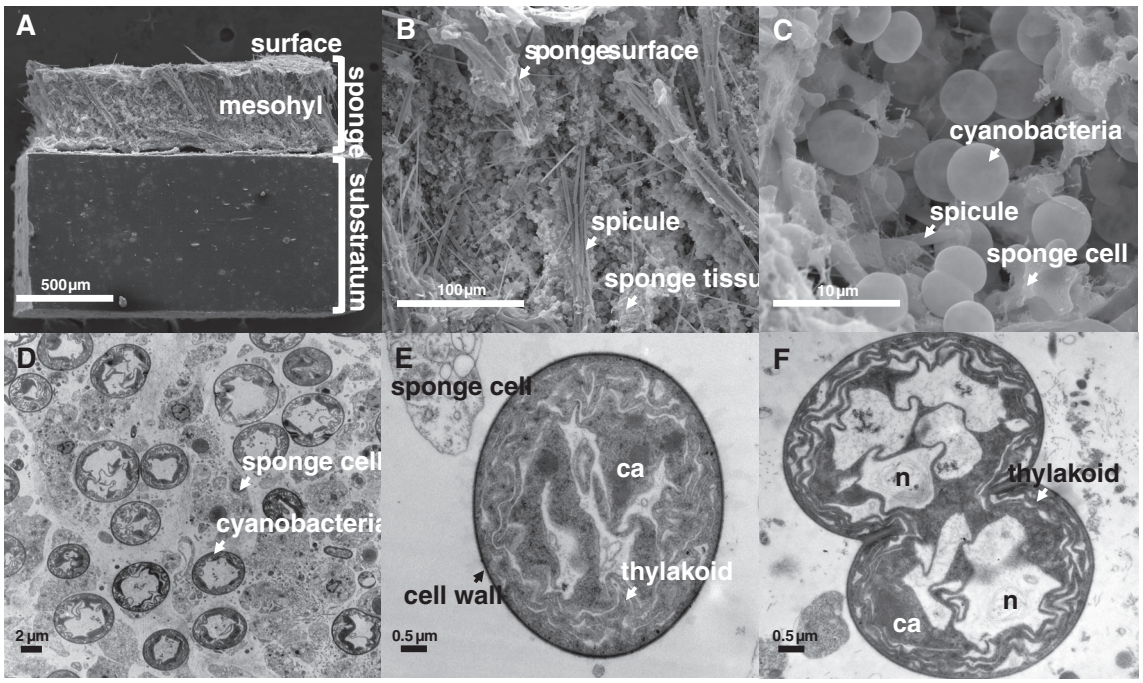

Fig 3. Electron micrographs of *T. hoshinota* and associated cyanobacteria.
A–C. SEM.
D and F. TEM.
A. Sponge covering an abiotic substratum. The sponge's skeleton was arranged in a tangential style, and the mesohyl was supported by a tract of spicules.
B and C. Close view of the mesohyl. Numerous spheres composing the inside of the mesohyl, and cross matched with (D); their thylakoids identified the spheres as cyanobacteria. The detailed structures of the cyanobacteria were observed from a single cyanobacterial cell (E) and a dividing cell (F); they included the cell wall, thylakoid, carboxysome (ca), and nucleoid (n).

Phylogenetic and functional genomic analyses revealed distinct characteristics of LD05 and SP5CPC1 genomes compared to other Prochloron *genomes*

Phylogenetic, genomic, and functional genomic analyses showed that LD05 and SP5CPC1 had distinct characteristics compared to *Prochloron*, suggesting that LD05 and SP5CPC1 should be classified into a genus other than *Prochloron*. LD05 and SP5CPC1 had smaller genomes but similar coding densities to other phylogenetically closely related cyanobacteria (Supporting Information - Table S3). In contrast, *Prochloron* had similar genome sizes (Wilcoxon Rank-Sum test, two-sided: $P = 0.07$) but a lower coding density (Wilcoxon Rank-Sum test, one-sided: $P = 0.002$). A phylogenetic tree of 120 cyanobacteria was constructed based on 120 single-copy genes to determine their phylogenetic affiliations (Fig. 5A and Fig. S4). The tree demonstrated that LD05 and SP5CPC1 formed a clade that was sister to that containing *P. didemni*. The larger clade encompassing the two clades was adjacent to the clade containing *Synechocystis*, *Myxosarcina*, and other cyanobacteria.

To provide an in-depth view, homologues of the LD05 16S rRNA gene with high similarities were retrieved from the NCBI database. A tree constructed using these 16S rRNA gene sequences depicted two distinct clades, referred to as Clade I and Clade II (Fig. 5B). Clade II contained 16S rRNA gene sequences from three genomes of *P. didemni* strains and other 16S rRNA gene sequences from various ascidians. In contrast, Clade I mainly comprised sequences from sponge holobionts, including SP5CPC1, LD05, and 16S rRNA gene sequences from a variety of other sponges. Although many sequences in Clade I were assigned as *Synechocystis* and *Prochloron* 16S rRNA gene sequences, we found that they shared greater identities with the members of Clade I than *Synechocystis* or *Prochloron didemni*. Moreover, phylogenomic analyses also revealed that SP5CPC1 and LD05 were phylogenetically distant from the cultivated *Synechocystis* (Fig. 5A).

Functional genomic analyses revealed that the characteristics of LD05 and SP5CPC1 were inconsistent with the hallmarks of *Prochloron*. We found that genes encoding phycobilin synthases and phycobiliproteins (i.e. phycoerythrin, phycocyanin, and allophycocyanin) were present in LD05 and SP5CPC1 but not in the *Prochloron* genomes. The absence of the chlorophyll *b* synthase gene in the LD05 and SP5CPC1 genomes implied that the bacteria lacked chlorophyll *b*. In addition,

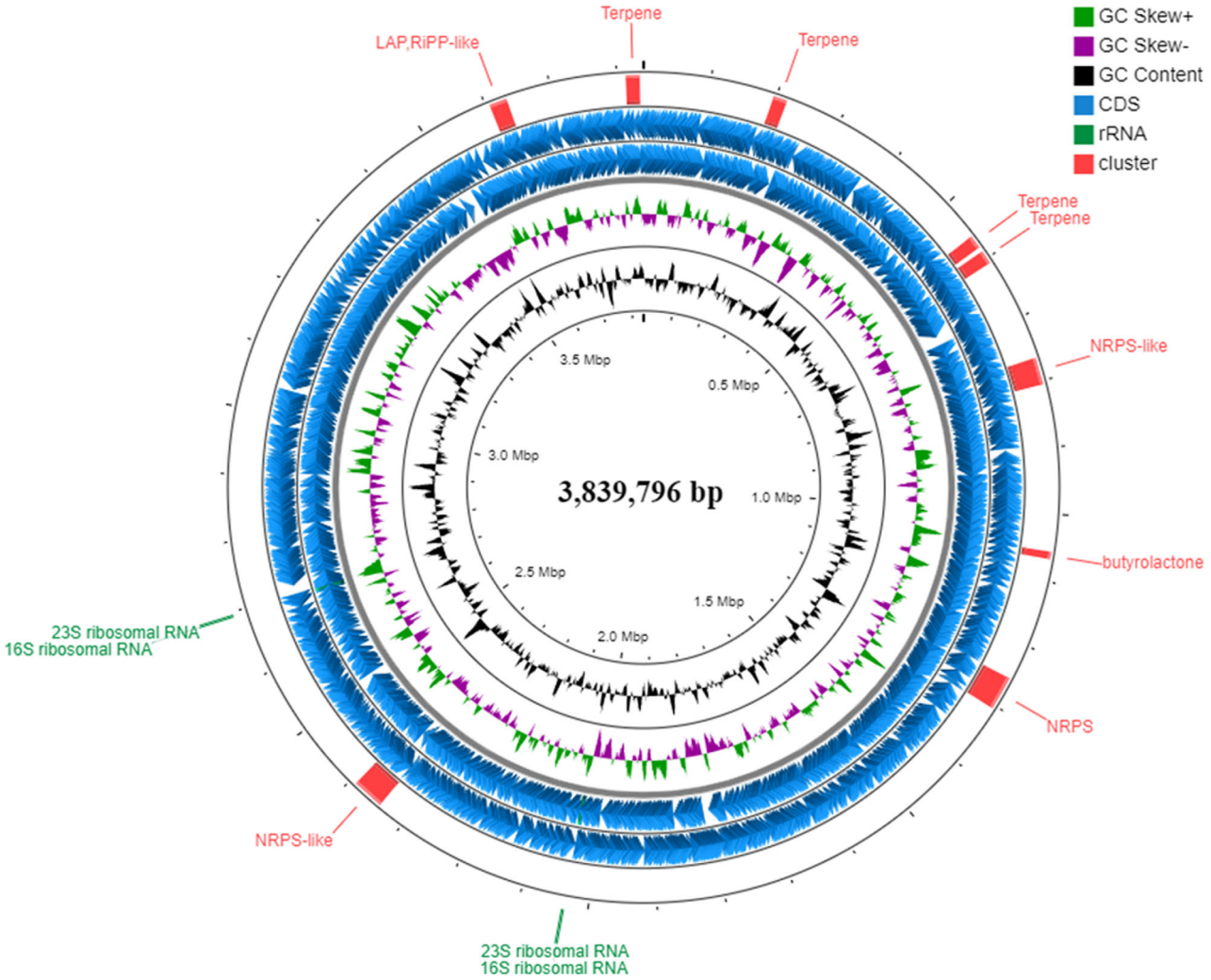

Fig 4. Representation of the 'Paraprochloron terpiosi LD05' genome.
The genome is 3 839 796 bp. The rings from inside to outside represent GC content (black), GC skew- (purple), GC skew + (green), coding sequence regions (blue), rRNA gene sequences (dark green), and secondary metabolite gene clusters (red).

Table 2. Basic statistics of the *Candidatus* Paraprochloron terpiosi LD05.

Candidatus Paraprochloron terpiosi LD05	
Closest species	*Prochloron didemni*
Average nucleotide identity to closest species (%)	77.97
Genome size (bp)	3839 796 bp
# contigs	1
GC content (%)	44.5
# predicted CDS	4102
Coding density (%)	82.4
tRNA	46
16S rRNA	2
23S rRNA	2

the failure to identify chlorophyll *b* in the ascidian *Tridemnum nubilum* holobiont, from which PCR clone AO15 (DQ357958.1) in Clade I was recovered, implyies that the bacterium also lacks chlorophyll *b*. In accordance with genomic analyses, our pigment analysis by LC-QTOF-MS also revealed the presence of chlorophyll *a* and the absence of chlorophyll *b* in *T. hoshinota* (Fig. 6). These results indicate that the bacteria in Clade I have different light-harvesting systems to those of *Prochloron* in Clade II.

The bacterial species in Clade I have a photosynthetic machinery distinct from that of *Prochloron*. The existence of phycobiliproteins and a lack of chlorophyll *b* were inconsistent with the definition of *Prochloron*. Therefore, we propose that bacteria in Clades I and II should be

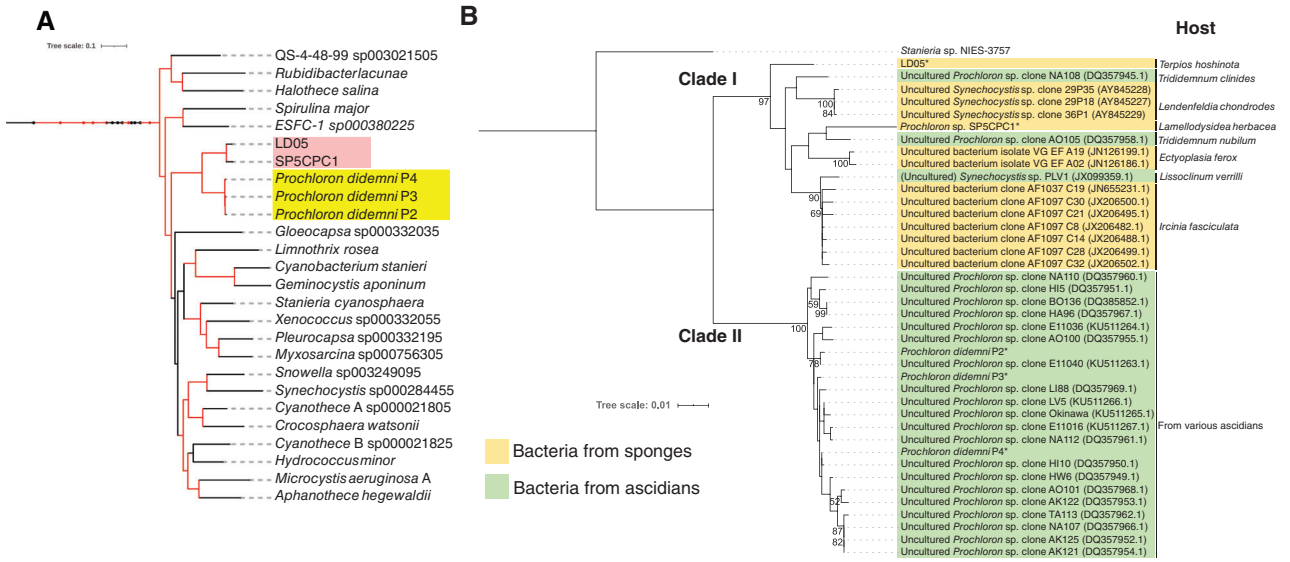

Fig 5. Molecular phylogenetic analyses of *Prochloron* and *Prochloron*-related bacteria.
A. Pruned phylogenetic tree based on the concatenation of 120 single-copy gene protein sequences. The complete phylogenetic tree including other cyanobacterial genera can be found in the Supporting Information Fig. S5. The branches with Ultrafast bootstrap (UFBoot) value >95% are highlighted with the red. The *Prochloron* genomes are labelled with yellow, and LD05 and SP5CPC1 are labelled with pink. *Vampirovibrio chlorellavorus* C was used as the outgroup.
B. A phylogenetic tree was constructed using the 16S rRNA gene by the maximum-likelihood method with 1000 bootstraps. The tree included 16S rRNA gene sequences from SP5CPC1, LD05, *Prochloron* genomes—including *P. didemni* P2, *P. didemni* P3, and *P. didemni* P4—and other related 16S rRNA gene sequences identified by PCR cloning from environmental samples. The 16S rRNA gene sequence of *Stanieria* sp. NIES-3757 genome was used as an outgroup. The scale bar represents the number of changes per nucleotide. Asterisk represents genomes that are available.

classified into two different genera and classify the species in Clade I as a novel genus 'Paraprochloron.' Moreover, we classified LD05 as a novel species named *Candidatus* Paraprochloron terpiosi LD05 [Etymology: Gr. pref. *para*-, beside, alongside of; N.L. neut. n. *Prochloron*, a bacterial generic name; N.L. neut. n. *Paraprochloron*, a genus adjacent to *Prochloron*. N.L. gen. n. *terpiosi*, of *Terpios* a zoological scientific genus name.].

Metabolic features of novel species Ca. *Pp. terpiosi LD05*

Ca. Pp. terpiosi LD05 possessed nearly all genes required for photosynthesis, carbon fixation, the tricarboxylic acid cycle (TCA), and glycolysis (Fig. 7). In addition, genes related to sucrose metabolism – e.g., sucrose-6-phosphatase, sucrose synthase, and sucrose phosphorylase – were identified. These genes were also present in the SP5CPC1 genome but not in *P. didemni* genomes (Supporting Information Table S4). Regarding nitrogen metabolism, the *Ca*. Pp. terpiosi LD05 and SP5CPC1 lacked nitrogen fixation genes. *Ca*. Pp. terpiosi LD05 had genes for nitrate uptake and assimilatory nitrate reduction pathways to convert nitrate into ammonium (Supporting Information Table S4). The glutamine synthetase/glutamate synthase (GS/GOGAT) pathway was also found in *Ca*. Pp. terpiosi LD05, indicating that ammonium derived from extracellular nitrate can be incorporated into amino acids via this pathway. Additionally, *Ca*. Pp. terpiosi LD05 carried the complete gene set for the urea transporter and urease. Bacteria can utilize urea transporter and urease to covert extracellular urea into ammonium as a nitrogen source. Besides these pathways of nitrogen acquisition, general L-amino acid transporters were identified in *Ca*. Pp. terpiosi LD05, which was not observed in the *Prochloron* genomes.

Genes participating in B-vitamin biosynthesis were found in *Ca*. Pp. terpiosi LD05 and SP5CPC1. *Ca*. Pp. terpiosi LD05 and SP5CPC1 genomes contained nearly the complete gene sets for synthesis pathways of vitamin B_1 (thiamine), vitamin B_2 (riboflavin), vitamin B_7 (biotin), and vitamin B_{12} (Supporting Information Table S4). The transporter for cobalt, a key constituent of vitamin B_{12}, was also identified. In contrast, *Prochloron* genomes lack a cobalt transporter gene and many genes involved in vitamin B_{12} synthesis.

Putative secondary metabolic gene clusters were found in the genomes of LD05 and SP5CPC1. Our analysis revealed the presence of four terpene synthesis gene clusters in *Ca*. Pp. terpiosi LD05 and SP5CPC1. Furthermore, LD05 also contains a gene encoding squalene

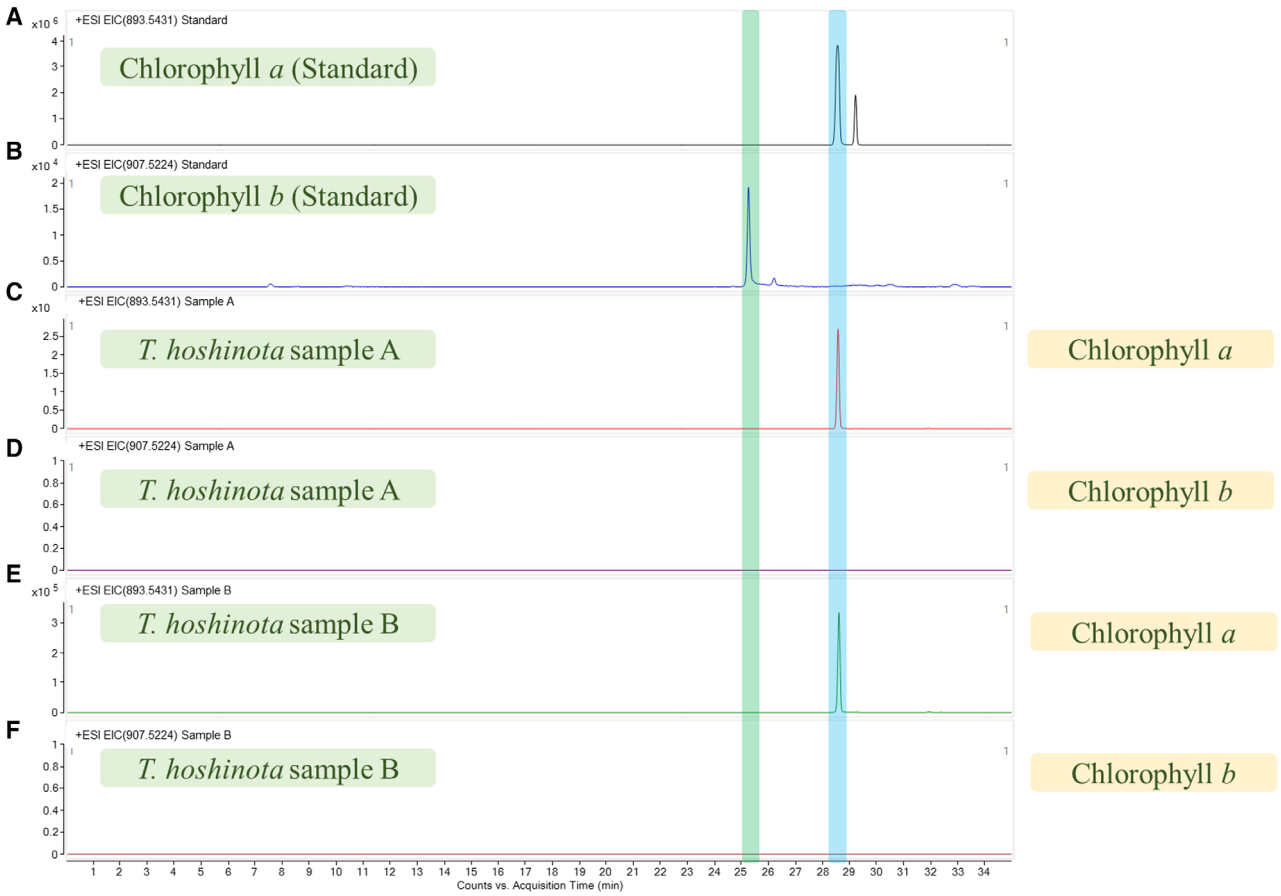

Fig 6. Extracted ion-chromatograms (EICs) of UPLC-QTOF-MS of the extracts of *T. hoshinota*. Chlorophyll *a* analytical standard (A) and chlorophyll *b* analytical standard (B) were used in the analysis. The analysis included two *T. hoshinota* samples. EIC of MS spectra within the m/z value of 893.543 (A, C, and E) and 907.522 (B, D, and F). A: chlorophyll *a* peak. B: chlorophyll *b* peak.

cyclase, suggesting that LD05 can produce cyclic triterpenes. Other secondary metabolite biosynthetic gene clusters were identified. Gene clusters present in *Ca*. Pp. terpiosi LD05 included butyrolactone, linear azol(in)e-containing peptides, and non-ribosomal peptide synthetase clusters (Fig. 4).

Symbiotic signatures and unique genomic features of Ca*. Pp. terpiosi LD05*

The complete genome of *Ca*. Pp. terpiosi LD05 enabled us to investigate genomic features in a precise and comprehensive manner. When we compared the LD05 and SP5CPC1 genomes with other phylogenetically close cyanobacteria, we found that *Ca*. Pp. terpiosi LD05 and SP5CPC1 lacked the *dnaA* gene, which encodes a protein for a replication initiation factor responsible for DNA unwinding at *oriC* (Katayama *et al*., 2010). By comparing the numbers of each KEGG orthology in the genomes, we found that *Ca*. Pp. terpiosi LD05 bacteria had 50 copies of RNA-directed DNA polymerase genes, which were not observed in other phylogenetically close cyanobacteria. Symbiotic bacteria often have high transposase content. In our analyses, we found that LD05 and SP5CPC1 had 39 and 31 predicted genes, respectively, annotated as transposases, while *Prochloron* genomes had 52–82 copies of transposase genes.

Discussion

T. hoshinota is one of the most important biological threats to corals in the Indo-Pacific region. Its association with cyanobacteria and other symbiotic bacteria is essential for maintaining the function of *T. hoshinota*. Our study is the first to explore the composition and role of the *T. hoshinota* microbiome. An unprecedented large-scale survey of the bacterial community of *T. hoshinota* based on 16S rRNA gene amplicon sequencing of samples from various regions across the western Pacific Ocean, Indian

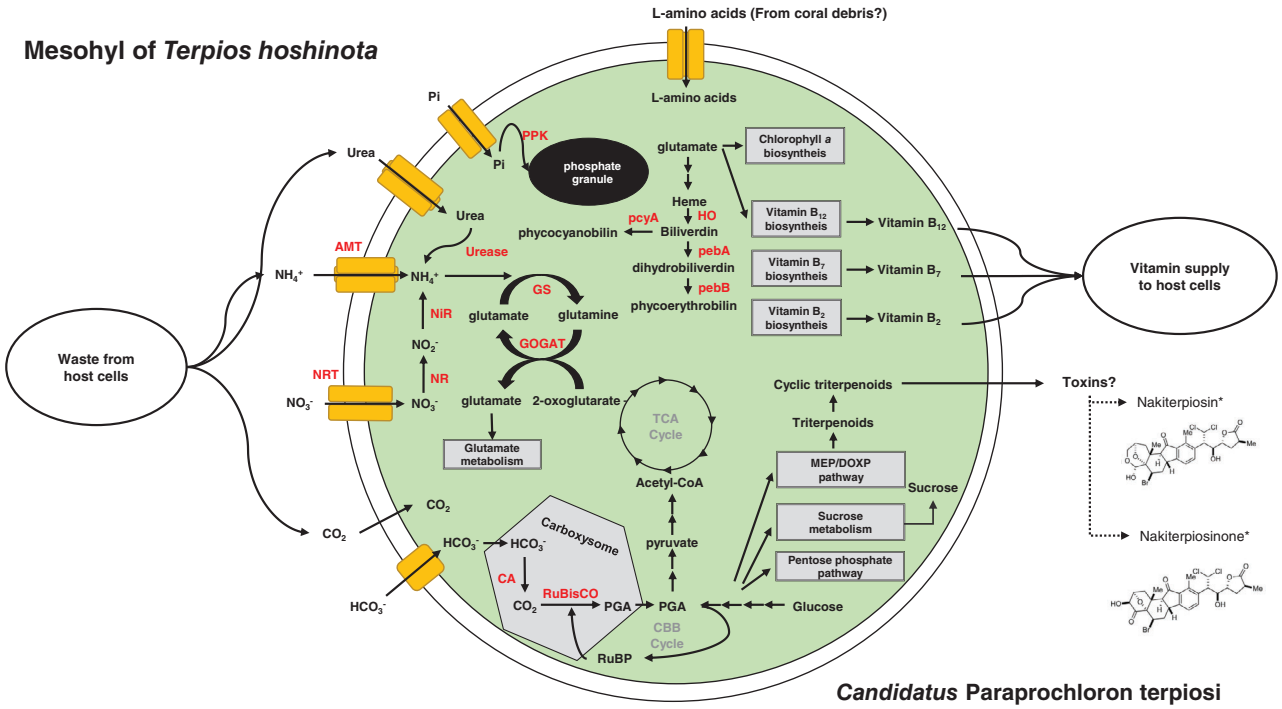

Fig 7. Metabolic potentials and putative nutrient cycling between *T. hoshinota* and *Ca*. Pp. terpiosi LD05.
The bacterium may recycle nitrogen waste from host cells and provide them with vitamins. The bacterium may also produce secondary metabolites as toxins to help the sponge weaken coral tissues and facilitate overgrowth. On the other hand, the bacterium may also store phosphate as an energy reservoir for the holobiont to prepare for the competition with coral. amt, ammonia transporter; NRT, nitrate transporter; NR, nitrate reductase; NiR, ferredoxin--nitrite reductase; CA, carbonic anhydrase; PPK, polyphosphate kinase; GS, glutamine synthetase; GOGAT, glutamine oxoglutarate aminotransferase; RuBisCo, ribulose-1,5-bisphosphate carboxylase/oxygenase; pcyA, phycocyanobilin:ferredoxin oxidoreductase; HO, heme oxygenase; pebA, dihydrobiliverdin:ferredoxin oxidoreductase; pebB, phycoerythrobilin:ferredoxin oxidoreductase. *The structures of nakiterpiosin and nakiterpiosinone are depicted based on Gao et al (2012).

Ocean, and South China Sea enabled us to characterize the *T. hoshinota* microbiome.

Biogeographical variation in the T. hoshinota *microbiome and its core microbial members*

Certain sponges exhibit high microbiome stability due to strict selective pressures exerted by their hosts. For instance, *Ircinia* and *Hexadella* sponges exhibit host-specificity and stability in their associated bacterial communities, despite large geographic distances between sampling sites (Pita *et al*., 2013; Reveillaud *et al*., 2014). In contrast, certain sponges, such as *Petrosia ficiformis*, harbour biogeography-dependent bacterial compositions (Burgsdorf *et al*., 2014).

Our survey of *T. hoshinota* from three oceans enabled us to determine whether bacterial communities of *T. hoshinota* vary across different biogeographical backgrounds or experience strong selective pressure from their hosts. The dissimilarity analysis of the microbial community structures of *T. hoshinota* showed a correlation between sample sites and microbial community structure (Fig. 1). The differences in microbial community structures among *T. hoshinota* samples from different locations may be the result of local acclimatization. Samples from the same regions may represent holobionts with similar metabolic functions to cope with stress or increased fitness in certain environments.

However, despite biogeographical variation, we still identified core bacterial members that were present in all samples (Table 1 and Fig. S2). This core bacterial community comprised only a few genera but accounted for around 80% of relative abundance across all samples, indicating that it is vital to the holobiont of *T. hoshinota*. Host-related factors may help keep this core microbiome stable because its members carry out core functions of the holobiont (Pita *et al*., 2018). Such core members may have the metabolic capability to utilize nutrients from the sponge host environment and play important roles in nutrient exchange, such as sulfur, carbon, and nitrogen cycling. This core group may also be responsible for defence against predators and for protecting sponge symbionts from toxins and pathogens (Pita *et al*., 2018).

The most dominant ASV in the core microbiome is closely related to *Prochloron*, a genus of symbiotic cyanobacteria found in various ascidians (Whatley, 1977; Kuhl *et al*., 2012). The biogeographically independent prevalence and predominance of this *Prochloron*-related

bacterium in *T. hoshinota* suggests that it plays a crucial role in the holobiont. On the other hand, symbiotic cyanobacteria in sponges can exhibit host specificity (Thacker and Starnes, 2003) or co-exist with various sponges (Konstantinou *et al*., 2018). The *Prochloron*-related ASV in *T. hoshinota* has not been observed in other organisms, implying that this *Prochloron*-related cyanobacterium may have high host specificity.

Candidatus *Paraprochloron terpiosi gen. nov., sp. nov., a* Prochloron*-related bacterium prevalent in* T. hoshinota

LD05 and SP5CPC1, two *Prochloron*-related bacteria in sponges, are distinct from *Prochloron* in terms of pigment content, phylogenetic divergence, and genomic features. Moreover, the pigment features of these bacteria are inconsistent with the definition of *Prochloron*. Hence, a new genus, 'Paraprochloron', is herein proposed to distinguish between these two groups.

Candidatus Paraprochloron terpiosi LD05 was the dominant cyanobacterium in *T. hoshinota* specimens collected across three different oceans (Supporting Information Table S2). Why the dominant cyanobacterium species remain identical in *T. hoshinota* across different oceans is unclear. Recent studies suggest that *T. hoshinota* larvae, which carry vertically transmitted cyanobacteria, may have short dispersal distances because they are denser than the water, leading them to settle rapidly after leaving their mother sponge (Wang *et al*., 2012a; Hsu *et al*., 2013; Nozawa *et al*., 2016). Under these circumstances, the symbiotic *Ca*. Pp. terpiosi LD05 from various locations might accumulate genetic differences to adapt to local environments. The absence of evident speciation in our study may be the result of tight and stable symbiotic interactions between *Ca*. Pp. terpiosi LD05 and *T. hoshinota*, which restrict genetic changes in the bacterium. Another possibility is that the species becomes broadly dispersed through other mechanisms, such as ocean currents or transportation via vessels, which would enable *T. hoshinota* larvae to spread quickly across oceans with few genetic alterations. Evidence of recent *T. hoshinota* outbreaks supports the latter scenario (Liao *et al*., 2007).

Comparison between 'Paraprochloron' and Prochloron

Comparative genomics involving 'Paraprochloron' and *Prochloron* enables us to infer their evolutionary histories and respective relationships with their hosts. Previous studies have shown that symbiotic bacteria usually have reduced genomes because certain genes erode as symbiosis develops (Gao *et al*., 2014; Lo *et al*., 2016). Furthermore, a model of symbiont evolution has proposed that during the evolutionary history of symbiosis, large-scale pseudogenization can occur during transitional events, such as strict host association or vertical transmission, leading to a sudden decrease in coding density (Lo *et al*., 2016). Eventually, the coding density gradually bounces back owing to deletion bias.

'Paraprochloron' had a comparatively smaller genome, while *Prochloron* had lower coding density compared to other phylogenetically closely related cyanobacteria (Supporting Information Table S3). These distinct genomic features between *Prochloron* and 'Paraprochloron' may indicate that the transition toward host-restricted lifestyles occurred more recently in *Prochloron* than in 'Paraprochloron'. This hypothesis may be supported by our observation that *Prochloron* harboured more transposase genes as the elevation of mobile genetic element quantities, such as transposons and insertion elements, which is thought to be associated with recent transition to a host-restricted symbiotic lifestyle (Moran *et al*., 2008).

Another hallmark of *Prochloron* is its ability to produce patellamides and cytotoxic cyclic peptides. However, a gene cluster for the synthesis of patellamides was not found in *Ca*. Pp. terpiosi LD05 or SP5CPC1. In contrast, the LD05 and SP5CPC1 genomes have four terpene synthesis gene clusters, whereas *Prochloron* genomes harbour only two such gene clusters. Moreover, LD05 and SP5CPC1 genomes contain genes encoding terpene cyclases, enzymes that catalyze the cyclization of linear terpenes. This indicates that LD05 and SP5CPC1 have cyclic terpenes. Taken together, 'Paraprochloron' and *Prochloron* may produce distinct secondary metabolites to increase the fitness of themselves or of their entire holobiont.

Certain cyanobacteria contain genes involved in sucrose metabolism. Although the role of sucrose in cyanobacteria remains understudied, several studies have shown that sucrose can be utilized as a compatible solute, serve as a signal molecule, or be employed for glycogen synthesis (Blumwald and Telor, 1982; Desplats *et al*., 2005; Curatti *et al*., 2008; Kolman *et al*., 2015). Interestingly, our genomic analysis revealed that the genes involved in sucrose metabolism were present in *Ca*. Pp. terpiosi LD05 and SP5CPC1 but absent in *Prochloron* (Supporting Information Table S4). We hypothesize that 'Paraprochloron' can use sucrose as an osmolyte to cope with osmotic stress; this is supported by a previous finding that the genes related to osmotic stress are found in sponge-associated bacterial genomes (Webster and Thomas, 2016). On the other hand, we also found that *Ca*. Pp. terpiosi LD05 and SP5CPC1 contained osmoprotectant transporter genes, which were not identified in *Prochloron* genomes (Supporting Information Table S4). These results indicate that the 'Paraprochloron' species may live in environments with higher osmotic stress, such as locations with high

osmolarity or fluctuations in osmolarity, compared to *Prochloron*. Alternatively, 'Paraprochloron' and *Prochloron* may use different strategies to deal with osmotic stress. Another possible role of sucrose is that 'Paraprochloron' may provide cells of sponge hosts or other symbiotic bacteria with sucrose as an energy or carbon source to promote the growth of sponge holobionts.

Another observation that drew our attention was the absence of the *dnaA* gene in *Ca*. Pp. terpiosi LD05 and SP5CPC1. DnaA is required for the initiation of DNA replication at *oriC* (Katayama *et al*., 2010). Some bacterial symbionts do not possess the *dnaA* gene and have multiple copies of the same genome in a single cell (Akman *et al*., 2002; Ran *et al*., 2010; Ohbayashi *et al*., 2016). The evolution of DnaA-independent replication has been most extensively studied in cyanobacteria. A study showed that cyanobacteria lost DnaA dependency before becoming symbiotic bacteria, and such loss can drive free-living bacteria to become symbiotic (Ohbayashi *et al*., 2016; Ohbayashi *et al*., 2020). However, in our analyses, *Prochloron* had *dnaA*, but 'Paraprochloron' did not, indicating the loss of *dnaA* occurred after the two bacteria separated from a common ancestor. This implies that symbiosis may also drive bacteria to lose *dnaA*.

Symbiotic interactions between Ca*. Pp. terpiosi and* T. hoshinota

The predominance of *Ca*. Pp. terpiosi LD05 highlights its role in *T. hoshinota*. Many sponges harbour photosynthetic symbionts that provide their host with nutrients (Erwin and Thacker, 2007; Thacker *et al*., 2007). Some sponges acquire >50% of their energy demand from symbiotic cyanobacteria in the form of photosynthates (Wilkinson, 1983; Taylor *et al*., 2007; Usher, 2008). Photosynthesis was observed in the *T. hoshinota* holobiont, and its efficiency increased when the coral-killing holobiont came into contact with coral, which may help sponges overgrow corals (Wang *et al*., 2015). As the dominant cyanobacteria, *Ca*. Pp. terpiosi LD05 may be an important carbon source for *T. hoshinota* and may facilitate competition with corals.

Certain symbiotic cyanobacteria in sponges can fix nitrogen (Wilkinson and Fay, 1979). *Ca*. Pp. terpiosi LD05 does not harbour genes related to nitrogen fixation, but genes related to ammonium transporters and the GS-GOGAT pathway were identified in *Ca*. Pp. terpiosi LD05, indicating that it could recycle ammonium from the cells of *T. hoshinota* in the mesohyl. On the other hand, *Ca*. Pp. terpiosi LD05 harbours urea transporter and urease genes. Therefore, urea can be used as an alternative nitrogen source. A previous study showed that levels of free amino acids in *T. hoshinota*-inhabiting cyanobacteria were elevated when the holobiont encountered a coral (Wang *et al*., 2015). Our finding of an amino acid transporter in *Ca*. Pp. Terpiosi LD05 suggests that the bacterium may benefit from 'coral killing' by consuming amino acids or ammonium that are released as coral colonies disintegrate.

Animals cannot synthesize essential vitamins, so symbiotic microorganisms are thought to be important sources of essential vitamins for sponges. Our analysis of the *Ca*. Pp. terpiosi LD05 genome identified biosynthetic pathways for vitamin B_1, vitamin B_7, and vitamin B_{12}. Thus, *Ca*. Pp. terpiosi LD05 may help maintain *T. hoshinota* health by providing the holobiont with vitamins.

One of the leading questions in the study of *T. hoshinota* is how it kills corals. Several mechanisms have been proposed to explain this. One argument is that the sponge produces cytotoxic allelochemicals that damage coral cells (Bryan, 1973). Another suggests that the sponge overgrows corals and competes with them for nutrients (Wang *et al*., 2012b). These hypotheses are not mutually exclusive. Several cytotoxic compounds, including nakiterpiosin, nakiterpiosinon, and terpiodiene, have been isolated from *T. hoshinota* holobionts (Teruya *et al*., 2002; Teruya *et al*., 2004). Nakiterpiosin and nakiterpiosinon are C-nor-D-homosteroids. Previous studies have shown that cyanobacteria can produce sterols by cyclization of squalene, a triterpene (Fagundes *et al*., 2019). In the *Ca*. Pp. terpiosi LD05 genome, biosynthetic pathways for squalene and squalene cyclases were identified. Hence, *Ca*. Pp. terpiosi LD05 may be responsible for toxin production. These toxins may facilitate the overgrowth of corals by damaging coral tissues directly or by weakening coral defences. In the future, the products of these gene clusters may be confirmed using molecular approaches.

Conclusions

This study makes several discoveries about bacterial communities associated with *T. hoshinota*. First, the study showed that although bacterial communities are governed by biogeography, four ASVs were prevalent in *T. hoshinota* and formed the core microbiome. The core microbiome of *T. hoshinota* includes a *Prochloron*-like bacterium, *Endozoicomonas*, SAR116, *Ruegeria*, and other unclassified *Proteobacteria*. Second, we found that the *Prochloron*-like bacterium was the predominant cyanobacterium in cyanobacteriosponge *T. hoshinota* and was present in all the samples and accounted for 30% relative read abundance on average, suggesting that this particular cyanobacterium is a potential obligate symbiont of the sponge. By genomic, phylogenetic, and pigment analyses, we found that LD05 and SP5CPC1 formed a sister clade adjacent to *Prochloron*, and they lack

chlorophyll *b* and have phycobilins, which is inconsistent with the definition of *Prochloron*. Hence, we propose the new genus 'Paraprochloron' to accommodate this clade. Third, we demonstrated that 'Paraprochloron' has genomic features distinct from those of *Prochloron*. 'Paraprochloron' has much smaller genomes, higher coding gene densities, and uses dnaA-independent DNA replication. In summary, our research will help future studies explore the detailed ecosystem inside the holobiont, and the complete genome reconstruction of *Ca*. Pp. terpiosi LD05 will help to extend our knowledge of cyanobacteria evolution and the functional diversity of symbiotic cyanobacteria.

Materials and methods

Sample collection

Sixty-one sponge samples, summarized in Supporting Information Table S1, were collected from 15 coastal sites in the western Pacific Ocean, South China Sea, and Indian Ocean by scuba diving. Before DNA isolation, sponge tissues were collected with tweezer underwater and placed in Falcon 50 ml conical centrifuge tubes. Samples were then washed with 1 ml of 1× TE buffer. The samples were fixed with 100% ethanol and stored at −20°C.

DNA extraction

For sponge samples from JPBS, JPISG, JPMYK, JPOKE, TWLD, TWLY, and USGU, total DNA was extracted using a DNeasy Blood and Tissue kit (QIAGEN, Hilden, Germany) according to the manufacturer's protocol. For the remaining samples, total DNA was extracted using a modified CTAB method described in our previous study (Tang *et al*., 2011). Tissue samples in alcohol were centrifuged at 14 000 × *g*. The supernatant was removed, and the pellet was incubated with 1 ml of 1× TE buffer three times. The pellet was resuspended in 500 μl TE buffer containing 30 μl 10% SDS and 3 μl 20 mg ml^{-1} protease K. The samples were maintained at 37°C for 1 h, followed by the addition of 100 μl of 5 M NaCl and 80 μl of CTAB/NaCl solution (i.e. 4% NaCl and 10% CTAB). The samples were kept at 65°C for 10 min, and the supernatant was transferred into sterilized tubes and treated with 600 μl of chloroform/isoamyl alcohol (24:l) solution. After gentle shaking for 1 min, the samples were centrifuged at 14 000 × *g* for 5 min at 4°C. The upper aqueous phase was transferred to a fresh tube with the addition of an equal volume of phenol/chloroform/isoamyl alcohol (25:24:1). The samples were centrifuged at 14 000 × *g* for 5 min at 4°C, and the supernatant was transferred to a new tube. DNA was precipitated with 0.6 volumes isopropanol. The mixture was centrifuged at 14 000 × *g* for 15 min, and the supernatant was discarded. The pellet was washed with 70% pre-chilled ethanol, air-dried, and resuspended in sterilized Milli-Q water. DNA samples were stored at −80°C for subsequent experiments.

16S rRNA gene amplification and multiplex tag sequencing

High-throughput sequencing of the 16S rRNA hypervariable V6–V8 region was used to characterize bacterial community diversity and composition. V6–V8 sequences were amplified by PCR with forward primer 5'-AACG CGAAGAACCTTAC-3' and reverse primer 5'-GACG GGCGGTGWGTRCA-3' (Lane, 1991). PCR mixtures contained 33.5 μl of sterilized distilled water, 0.5 μl of 5 U TaKaRa Ex Taq (Takara Bio, Otsu, Japan), 5 μl of 10X Ex Taq buffer, 4 μl of 10 mM dNTP, 1 μl of each primer at a concentration of 10 μM, and 5 μl template DNA in a total volume of 50 μl. PCR was programmed with an initial step of 94°C for 5 min, 30 cycles of 94°C for 30 s, 52°C for 20 s, and 72°C for 30 s, followed by a final step of 72°C for 10 min. PCR was performed again to add barcodes to the amplicons. Each primer tag was designed with four extra nucleotides at the 5' end of both primers. Unique tags were used for PCR barcoding to label each sample in the study. PCR conditions were the same as that for the V6–V8 amplification, except that the number of reaction cycles was reduced to five. The products were purified by 1.5% agarose electrophoresis and QIAEX II Agarose Gel Extraction kit (QIAGEN, Hilden, Germany) according to manufacturer's instruction. The quality of the purified products was assessed using a Nanodrop spectrophotometer (Thermo Scientific, Waltham, USA).

Illumina DNA sequencing and community analysis

DNA concentrations were measured using a Quant-iT™ assay (Thermo Fisher Scientific). Equal pools of DNA were sent to Yourgene Bioscience (Taipei, Taiwan) and sequenced using the MiSeq platform (Illumina, San Diego, USA). Short and low-quality reads were filtered using Mothur v.1.38.1 (Schloss *et al*., 2009) to retain reads with an average quality score > 27 and length of 365–451 base pairs (bp). Reads with homopolymers >8 bp were excluded, and chimeric sequences from all samples were removed using USEARCH v8.1.1861 (Edgar, 2010). ASVs were determined using DADA2 on the QIIME2 platform (Callahan *et al*., 2016; Bolyen *et al*., 2019). ASVs were classified with reference to the Silva v128 database (Yilmaz *et al*., 2014) using Mothur.

ASVs assigned to Archaea, Eukaryota, chloroplasts, and mitochondria were removed.

Alpha and beta diversity analyses were performed on rarefied data using QIIME 2 v2020.6 (Bolyen *et al*., 2019). Alpha diversity indices were calculated using Shannon diversity, Chao1 richness estimator, and Faith's phylogenetic diversity. Dissimilarities in microbial community composition among samples were computed using Bray–Curtis distance dissimilarity, unweighted UniFrac, and weighted UniFrac. The results were visualized using dendrograms. To evaluate the effects of sampling sites on alpha and beta diversity, sites with sample numbers >2 were used to perform statistical tests. The associations between alpha diversity indices and sampling locations were tested using the Kruskal–Wallis test. PERMANOVA analysis was performed using the adonis function in R. PERMANOVA with 999 permutations was conducted to evaluate potential associations between sampling sites and microbial community structures based on Bray–Curtis distance, unweighted UniFrac, and weighted UniFrac metrics. To control for variations in microbial community caused by collection year, collection year was set as a blocking variable in 'strata' argument.

Electron microscopy

A *T. hoshinota* sample at the sponge-coral border was observed by TEM, and *T. hoshinota* encompassing a rubber tire was observed by SEM. Samples were prepared as described in our previous study (Tang *et al*., 2011). Samples were fixed in 0.1 M phosphate buffer with 2.5% glutaraldehyde and 4% paraformaldehyde. After fixation, the samples were washed with 0.1 M phosphate buffer for 15 min three times and immersed in 0.1 M phosphate buffer with 1% osmium tetroxide for 4 h.

For TEM, sample was washed again three times and sequentially dehydrated in acetone at 30%, 50%, 70%, 85%, 95%, and 100% for 20 min each time. After dehydration, the sample was embedded in Spurr's resin and sectioned. The section was stained with 5% uranyl acetate in methanol and 0.5% lead citrate. The stained sample was observed using a Philips CM-100 TEM instrument.

For SEM, sample was sequentially dehydrated in 30% for 1 h, 50% for 1 h 70% for 1 h, 85% for 2 h, 95% for 2 h, 100% for 2 h, and 100% for 12 h. The sample was dried in a Hitachi HCP-2, Crytical point dryer, gold coated with a Hitachi E-1010, and observed using an FEI Quanta 200 SEM.

Pigment analysis by UPLC-QTOF-MS

Approximately 2.5 g of wet *T. hoshinota* tissue from each sample was centrifuged at 2000 $\times$ *g* for 30 s to remove excess water. Sponge tissues were placed in mortars and ground with 4 ml of 100% acetone to homogenize the tissues. The homogeneous samples were transferred into a 5 ml centrifuge tube and centrifuged at 2000 $\times$ *g* at room temperature for 30 s. The supernatant was transferred into a new 5-ml centrifuge tube. The samples were covered with aluminium foil paper for being shaded and stored at 4°C until pigment analysis.

Pigment content analysis was performed by UPLC-MS. The UPLC-MS system used the Agilent 1290 Infinity II ultra-performance liquid chromatography (UPLC) system (Agilent Technologies, Palo Alto, CA, USA) coupled online to the Dual AJS electrospray ionization (ESI) source of an Agilent 6545 quadrupole time-of-flight (Q-TOF) mass spectrometer (Agilent Technologies). The samples were separated using a Kinetex XB-C18 column (2.6 μm, 4.6 $\times$ 100 mm, Phenomenex, Torrance, CA, USA) at 40°C. The chromatogram was acquired; mass spectral peaks were detected and their waveform processed using Agilent Qualitative Analysis 10.0 software (Agilent, USA).

Metagenome sequencing and assembly

Nanopore and Illumina sequencing were used to recover metagenome-assembled genomes (MAGs) with high accuracy. For Illumina sequencing, *T. hoshinota* tissues were ground, and the samples were filtered through a 35 μm nylon mesh (Falcon® 5 ml Round Bottom Polystyrene Test Tube, with Cell Strainer Snap Cap). A 1 $\times$ 10^8 cyanobacterial cells were purified from the samples using the MoFlo XDP cell sorter based on fluorescence and forward scatter intensity. The cells were then retained on a 0.2-μm cellulose acetate membrane filter, and the DNA was extracted by the modified CTAB method mentioned above. Purified DNA was sent to Yourgene Bioscience (Taipei, Taiwan) and sequenced on a MiSeq platform (Illumina, USA).

Nanopore sequencing was performed on *T. hoshinota* larvae. *T. hoshinota* larvae were searched on *T. hoshinota* adult by scuba diving around Gonguuan (22°40' N 121°27′ E) in Lyudao, Taiwan on 04 July 2020. Larvae were collected into a Falcon 50 ml conical centrifuge tube with a dropper underwater. The larvae were then selected into a Petri dish using a microscope to remove contamination, and the larvae were then fixed with absolute ethanol and stored at −20°C until DNA extraction. The total DNA was extracted by the modified CTAB method mentioned above. After DNA extraction, the DNA was sent to NGS Core at Biodiversity Research Center, Academia Sinica for Nanopore sequencing.

To recover cyanobacterial genome from the metagenome, nanopore reads were assembled by metaFlye with default settings (Kolmogorov *et al*., 2020). One

contig was annotated as circular by metaFlye, and it was assigned as a novel cyanobacterial species by the GTDB-TK taxonomy annotation (Chaumeil *et al*., 2020). Because nanopore reads are error-prone, the genome was polished by Illumina reads in order to increase the accuracy of the genome. First, Illumina reads were trimmed and filtered by trimmomatic v0.39 with the following parameters: ILLUMINACLIP:TruSeq3-PE-2.fa:2:30:10:3: TRUE LEADING:10 TRAILING:10 SLIDINGWINDOW:5:15 MINLEN:50 (Bolger *et al*., 2014). The processed reads were mapped to the cyanobacterial contig, and the contig was then polished with Pilon by the mapping result (Walker *et al*., 2014).

Genome annotation and analyses

The genome of *Prochloron*, 'Paraprochloron', and phylogenetically close cyanobacteria were annotated using Prokka v1.13.7 with the 'usegenus' and 'rfam' options (Seemann, 2014). The genomes were also annotated with KEGG functional orthologues (KO numbers) and clusters of orthologous (COGs) (Kanehisa and Goto, 2000; Tatusov *et al*., 2000). To annotate the KO numbers, protein sequences predicted by Prodigal were blasted against the KEGG prokaryotic species gene database with bacteria taxonomy group using BlastKoala (Hyatt *et al*., 2010; Kanehisa *et al*., 2016; Boyd *et al*., 2019). The KO number annotation results were then used to reconstruct the transporter systems and metabolic pathways using KEGG mapper (Kanehisa and Sato, 2020). To annotate Clusters of Orthologous (COGs), the predicted protein sequences were searched against the COG database by PSI-BLAST with an e-value threshold of 10^{-5} (Camacho *et al*., 2009). In addition, the transporter proteins were identified by searching the putative protein sequences against TransportDB 2.0 (August 2019) using BLASTp (Elbourne *et al*., 2017).

ANI calculation and phylogenetic analyses

The ANIs between genomes were determined using FastANI (Jain *et al*., 2018). To reconstruct a phylogenetic tree of the 16S rRNA genes, the sequences with high identities to the 16S rRNA gene in LD05 genome were retrieved by searching the NCBI nt database using BLASTn (Camacho *et al*., 2009; Coordinators, 2018). The sequences were aligned by MUSCLE on MEGA7 (Edgar, 2004; Kumar *et al*., 2016). A tree was then reconstructed using IQ-TREE v2.03 using automatic model selection and 1000 bootstraps (Minh *et al*., 2020). The tree was visualized with iTOL v4 (Letunic and Bork, 2019).

Genomes for each cyanobacteria species in GTDB database were downloaded and 120 single-copy gene protein sequences were used to reconstruct a tree (Parks *et al*., 2018). Marker gene protein sequences were identified, aligned, and concatenated by GTDB-TK v1.3.0 (Chaumeil *et al*., 2020). A phylogenomic tree was then built using IQ-TREE v2.03 with automatic model selection and 1000 Ultrafast bootstraps. The tree was visualized with iTOL v4 (Letunic and Bork, 2019; Minh *et al*., 2020).

Data Availability

All the raw data and genome were submitted under BioProject ID: PRJNA665642.

Acknowledgements

Y.H.C acknowledges the Taiwan International Graduate Program (TIGP) for its fellowship toward his graduate studies. The authors thank Noah Last of Draft Editing for his English language editing, Dr. Ker-yea Soong and Shih-Shou Fang for collecting *T. hoshinota* samples, and the Green Island Marine Research Station for supporting the research. The authors thank the electron microscope and flow cytometry divisions of IPMB, Academia Sinica for their technical support and Chih-Yu Lin and Gong-Min Lin in the Metabolomics Core Facility, Agricultural Biotechnology Research Center, Academia Sinica for the technical support and for performing the UPLC-MS/MS analysis and processing data. This work was funded by Biodiversity Research Center, Academia Sinica and the National Science Council, Taiwan (NSC98-2321-B-001-025-MY3678106).

Authors' contributions

Y.H.C., H.J.C., and S.L.T. designed the study and prepared the manuscript. Y.H.C. and H.J.C. analysed and interpreted the data. H.J.C., C.Y.Y., J.H.S., D.Z.H., P.W.C., M.H.L., and W.S.C. collected and sequenced the samples. H.J.C., C.Y.Y., and J.H.S. performed the electron microscopy. H.J.C., T.H.S., S.H.L., and C.M.Y. examined the pigments. C.A.C., J.D.R., E.H., B.H.I., H.H., P.J.S., C.H.J.T., and H.Y. assisted with the sampling. All authors read and approved the manuscript.

References

Akman, L., Yamashita, A., Watanabe, H., Oshima, K., Shiba, T., Hattori, M., and Aksoy, S. (2002) Genome sequence of the endocellular obligate symbiont of tsetse flies, Wigglesworthia glossinidia. *Nat Genet* **32**: 402–407.

Blumwald, E., and Telor, E. (1982) Osmoregulation and cell composition in salt-adaptation of Nostoc-Muscorum. *Arch Microbiol* **132**: 168–172.

Bolger, A.M., Lohse, M., and Usadel, B. (2014) Trimmomatic: a flexible trimmer for Illumina sequence data. *Bioinformatics* **30**: 2114–2120.

Bolyen, E., Rideout, J.R., Dillon, M.R., Bokulich, N., Abnet, C.C., Al-Ghalith, G.A., *et al*. (2019) Reproducible,

interactive, scalable and extensible microbiome data science using QIIME 2. *Nat Biotechnol* **37**: 852–857.
Boyd, J.A., Woodcroft, B.J., and Tyson, G.W. (2019) Comparative genomics using EnrichM, URL https://github.com/geronimp/enrichM (in preperation)
Bryan, P.G. (1973) Growth rate, toxicity and distribution of the encrusting sponge Terpios sp.(Hadromerida: Suberitidae) in Guam, Mariana Islands. *Micronesica* **9**: 237–242.
Burgsdorf, I., Erwin, P.M., Lõpez-Legentil, S., Cerrano, C., Haber, M., Frenk, S., and Steindler, L. (2014). Biogeography rather than association with cyanobacteria structures symbiotic microbial communities in the marine sponge Petrosia ficiformis. *Frontiers in Microbiology* **5**: 1–11.
Callahan, B.J., McMurdie, P.J., Rosen, M.J., Han, A.W., Johnson, A.J.A., and Holmes, S.P. (2016) DADA2: high-resolution sample inference from Illumina amplicon data. *Nature Methods* **13**: 581.
Camacho, C., Coulouris, G., Avagyan, V., Ma, N., Papadopoulos, J., Bealer, K., and Madden, T.L. (2009) BLAST plus: architecture and applications. *BMC Bioinformatics* **10**: 1–9.
Chaumeil, P.A., Mussig, A.J., Hugenholtz, P., and Parks, D. H. (2020) GTDB-Tk: a toolkit to classify genomes with the genome taxonomy database. *Bioinformatics* **36**: 1925–1927.
Coordinators, N.R. (2018) Database resources of the National Center for biotechnology information. *Nucleic Acids Res* **46**: D8–D13.
Curatti, L., Giarrocco, L.E., Cumino, A.C., and Salerno, G.L. (2008) Sucrose synthase is involved in the conversion of sucrose to polysaccharides in filamentous nitrogen-fixing cyanobacteria. *Planta* **228**: 617–625.
de Voogd, N.J., Cleary, D.F.R., and Dekker, F. (2013) The coral-killing sponge Terpios hoshinota invades Indonesia. *Coral Reefs* **32**: 755–755.
Desplats, P., Folco, E., and Salerno, G.L. (2005) Sucrose may play an additional role to that of an osmolyte in Synechocystis sp PCC 6803 salt-shocked cells. *Plant Physiol Biochem* **43**: 133–138.
Edgar, R.C. (2004) MUSCLE: a multiple sequence alignment method with reduced time and space complexity. *BMC Bioinformatics* **5**: 113.
Edgar, R.C. (2010) Search and clustering orders of magnitude faster than BLAST. *Bioinformatics* **26**: 2460–2461.
Elbourne, L.D.H., Tetu, S.G., Hassan, K.A., and Paulsen, I. T. (2017) TransportDB 2.0: a database for exploring membrane transporters in sequenced genomes from all domains of life. *Nucleic Acids Res* **45**: D320–D324.
Erwin, P.M., and Thacker, R.W. (2007) Incidence and identity of photosynthetic symbionts in Caribbean coral reef sponge assemblages. *J Mar Biol Assoc* **87**: 1683–1692.
Fagundes, M.B., Falk, R.B., Facchi, M.M.X., Vendruscolo, R. G., Maroneze, M.M., Zepka, L.Q., *et al*. (2019) Insights in cyanobacteria lipidomics: a sterols characterization from Phormidium autumnale biomass in heterotrophic cultivation. *Food Res Int* **119**: 777–784.
Fujii, T., Keshavmurthy, S., Zhou, W., Hirose, E., Chen, C., and Reimer, J. (2011) Coral-killing cyanobacteriosponge (Terpios hoshinota) on the great barrier reef. *Coral Reefs* **30**: 483–483.
Gao, Z.M., Wang, Y., Tian, R.M., Wong, Y.H., Batang, Z.B., Al-Suwailem, A.M., *et al*. (2014) Symbiotic adaptation drives genome streamlining of the cyanobacterial sponge symbiont "Candidatus Synechococcus spongiarum". *MBio* **5**: e00079-14.
Gao, S., Wang, Q., Wang, G., Lomenick, B., Liu, J., Fan, C. W., *et al*. (2012) The chemistry and biology of nakiterpiosin - C-nor-D-Homosteroids. *Synlett* **16**: 2298–2310. https://doi.org/10.1055/s-0031-1290460.
Hentschel, U., Piel, J., Degnan, S.M., and Taylor, M.W. (2012) Genomic insights into the marine sponge microbiome. *Nat Rev Microbiol* **10**: 641–U675.
Hirose, E., and Murakami, A. (2011) Microscopic anatomy and pigment characterization of coral-encrusting black sponge with cyanobacterial symbiont, Terpios hoshinota. *Zoolog Sci* **28**: 199–205.
Hoeksema, B.W., Waheed, Z., and de Voogd, N.J. (2014) Partial mortality in corals overgrown by the sponge Terpios hoshinota at Tioman Island, peninsular Malaysia (South China Sea). *Bull Mar Sci* **90**: 989–990.
Hsu, C.M., Wang, J.T., and Chen, C.A. (2013) Larval release and rapid settlement of the coral-killing sponge, Terpios hoshinota, at Green Island, Taiwan. *Mar Biodivers* **43**: 259–260.
Hyatt, D., Chen, G.L., LoCascio, P.F., Land, M.L., Larimer, F.W., and Hauser, L.J. (2010) Prodigal: prokaryotic gene recognition and translation initiation site identification. *BMC Bioinformatics* **11**: 1–11.
Jain, C., Rodriguez-R, L.M., Phillippy, A.M., Konstantinidis, K.T., and Aluru, S. (2018) High throughput ANI analysis of 90K prokaryotic genomes reveals clear species boundaries. *Nat Commun* **9**: 1–8.
Kanehisa, M., and Goto, S. (2000) KEGG: Kyoto encyclopedia of genes and genomes. *Nucleic Acids Res* **28**: 27–30.
Kanehisa, M., and Sato, Y. (2020) KEGG mapper for inferring cellular functions from protein sequences. *Protein Sci* **29**: 28–35.
Kanehisa, M., Sato, Y., and Morishima, K. (2016) BlastKOALA and GhostKOALA: KEGG tools for functional characterization of genome and Metagenome sequences. *J Mol Biol* **428**: 726–731.
Katayama, T., Ozaki, S., Keyamura, K., and Fujimitsu, K. (2010) Regulation of the replication cycle: conserved and diverse regulatory systems for DnaA and oriC. *Nat Rev Microbiol* **8**: 163–170.
Kolman, M.A., Nishi, C.N., Perez-Cenci, M., and Salerno, G. L. (2015) Sucrose in cyanobacteria: from a salt-response molecule to play a key role in nitrogen fixation. *Life (Basel)* **5**: 102–126.
Kolmogorov, M., Bickhart, D.M., Behsaz, B., Gurevich, A., Rayko, M., Shin, S.B., *et al*. (2020) metaFlye: scalable long-read metagenome assembly using repeat graphs. *Nat Methods* **17**: 1103–1110.
Konstantinou, D., Gerovasileiou, V., Voultsiadou, E., and Gkelis, S. (2018) Sponges-cyanobacteria associations: global diversity overview and new data from the eastern Mediterranean. *PLoS One* **13**: e0195001.
Kuhl, M., Behrendt, L., Trampe, E., Qvortrup, K., Schreiber, U., Borisov, S.M., *et al*. (2012) Microenvironmental ecology of the chlorophyll b-containing symbiotic

cyanobacterium prochloron in the Didemnid ascidian Lissoclinum patella. *Front Microbiol* **3**: 402.
Kumar, S., Stecher, G., and Tamura, K. (2016) MEGA7: molecular evolutionary genetics analysis version 7.0 for bigger datasets. *Mol Biol Evol* **33**: 1870–1874.
Lane, D. (1991) 16S/23S rRNA sequencing. *Nucl Acid Tech Bacterial Syst*: 115–175.
Letunic, I., and Bork, P. (2019) Interactive tree of life (iTOL) v4: recent updates and new developments. *Nucleic Acids Res* **47**: W256–W259.
Liao, M.-H., Tang, S.-L., Hsu, C.-M., Wen, K.-C., Wu, H., Chen, W.-M., *et al*. (2007) The" black disease" of reef-building corals at Green Island, Taiwan-outbreak of a Cyanobacteriosponge. Terpios hoshinota (Suberitidae; Hadromerida). *Zool Stud* **46**: 520.
Lo, W.S., Huang, Y.Y., and Kuo, C.H. (2016) Winding paths to simplicity: genome evolution in facultative insect symbionts. *FEMS Microbiol Rev* **40**: 855–874.
Madduppa, H., Schupp, P.J., Faisal, M.R., Sastria, M.Y., and Thoms, C. (2017) Persistent outbreaks of the "black disease" sponge Terpios hoshinota in Indonesian coral reefs. *Mar Biodivers* **47**: 149–151.
Minh, B.Q., Schmidt, H.A., Chernomor, O., Schrempf, D., Woodhams, M.D., von Haeseler, A., and Lanfear, R. (2020) IQ-TREE 2: new models and efficient methods for phylogenetic inference in the genomic era. *Mol Biol Evol* **37**: 1530–1534.
Montano, S., Chou, W.H., Chen, C.A., Galli, P., and Reimer, J.D. (2015) First record of the coral-killing sponge Terpios hoshinota in the Maldives and Indian Ocean. *Bull Mar Sci* **91**: 97–98.
Moran, N.A., McCutcheon, J.P., and Nakabachi, A. (2008) Genomics and evolution of heritable bacterial Symbionts. *Annu Rev Genet* **42**: 165–190.
Nozawa, Y., Huang, Y.S., and Hirose, E. (2016) Seasonality and lunar periodicity in the sexual reproduction of the coral-killing sponge, Terpios hoshinota. *Coral Reefs* **35**: 1071–1081.
Ohbayashi, R., Hirooka, S., Onuma, R., Kanesaki, Y., Hirose, Y., Kobayashi, Y., *et al*. (2020) Evolutionary changes in DnaA-dependent chromosomal replication in cyanobacteria. *Front Microbiol* **11**: 786.
Ohbayashi, R., Watanabe, S., Ehira, S., Kanesaki, Y., Chibazakura, T., and Yoshikawa, H. (2016) Diversification of DnaA dependency for DNA replication in cyanobacterial evolution. *ISME J* **10**: 1113–1121.
Parks, D.H., Chuvochina, M., Waite, D.W., Rinke, C., Skarshewski, A., Chaumeil, P.A., and Hugenholtz, P. (2018) A standardized bacterial taxonomy based on genome phylogeny substantially revises the tree of life. *Nat Biotechnol* **36**: 996.
Pita, L., Rix, L., Slaby, B.M., Franke, A., and Hentschel, U. (2018) The sponge holobiont in a changing ocean: from microbes to ecosystems. *Microbiome* **6**: 46.
Pita, L., Turon, X., Lopez-Legentil, S., and Erwin, P.M. (2013) Host rules: spatial stability of bacterial communities associated with marine sponges (Ircinia spp.) in the Western Mediterranean Sea. *FEMS Microbiol Ecol* **86**: 268–276.
Plucerrosario, G. (1987) The effect of substratum on the growth of Terpios, an encrusting sponge which kills corals. *Coral Reefs* **5**: 197–200.
Podell, S., Blanton, J.M., Oliver, A., Schorn, M.A., Agarwal, V., Biggs, J.S., *et al*. (2020) A genomic view of trophic and metabolic diversity in clade-specific Lamellodysidea sponge microbiomes. *Microbiome* **8**: 97.
Qin, Q.L., Xie, B.B., Zhang, X.Y., Chen, X.L., Zhou, B.C., Zhou, J., *et al*. (2014) A proposed genus boundary for the prokaryotes based on genomic insights. *J Bacteriol* **196**: 2210–2215.
Ran, L., Larsson, J., Vigil-Stenman, T., Nylander, J.A., Ininbergs, K., Zheng, W.W., *et al*. (2010) Genome erosion in a nitrogen-fixing vertically transmitted endosymbiotic multicellular cyanobacterium. *PLoS One* **5**: e11486.
Reveillaud, J., Maignien, L., Eren, A.M., Huber, J.A., Apprill, A., Sogin, M.L., and Vanreusel, A. (2014) Host-specificity among abundant and rare taxa in the sponge microbiome. *ISME J* **8**: 1198–1209.
Richter, M., and Rossello-Mora, R. (2009) Shifting the genomic gold standard for the prokaryotic species definition. *Proc Natl Acad Sci U S A* **106**: 19126–19131.
Rützler, K., and Muzik, K. (1993) Terpios hoshinota, a new cyanobacteriosponge threatening pacific reefs. *Scientia Marina* **57**: 395–403.
Schloss, P.D., Westcott, S.L., Ryabin, T., Hall, J.R., Hartmann, M., Hollister, E.B., *et al*. (2009) Introducing mothur: open-source, platform-independent, community-supported software for describing and comparing microbial communities. *Appl Environ Microbiol* **75**: 7537–7541.
Seemann, T. (2014) Prokka: rapid prokaryotic genome annotation. *Bioinformatics* **30**: 2068–2069.
Shi, Q., Liu, G., Yan, H.Q., and Zhang, H.L. (2012) Black disease (Terpios hoshinota): a probable cause for the rapid coral mortality at the northern reef of Yongxing Island in the South China Sea. *Ambio* **41**: 446–455.
Soong, K., Yang, S.L., and Chen, C.A. (2009) A novel dispersal mechanism of a coral-threatening sponge, Terpios hoshinota (Suberitidae, Porifera). *Zool Stud* **48**: 596–596.
Tang, S.L., Hong, M.J., Liao, M.H., Jane, W.N., Chiang, P. W., Chen, C.B., and Chen, C.A. (2011) Bacteria associated with an encrusting sponge (Terpios hoshinota) and the corals partially covered by the sponge. *Environ Microbiol* **13**: 1179–1191.
Tatusov, R.L., Galperin, M.Y., Natale, D.A., and Koonin, E.V. (2000) The COG database: a tool for genome-scale analysis of protein functions and evolution. *Nucleic Acids Res* **28**: 33–36.
Taylor, M.W., Radax, R., Steger, D., and Wagner, M. (2007) Sponge-associated microorganisms: evolution, ecology, and biotechnological potential. *Microbiol Mol Biol Rev* **71**: 295–347.
Teruya, T., Nakagawa, S., Koyama, T., Arimoto, H., Kita, M., and Uemura, D. (2004) Nakiterpiosin and nakiterpiosinone, novel cytotoxic C-nor-D-homosteroids from the Okinawan sponge Terpios hoshinota. *Tetrahedron* **60**: 6989–6993.
Teruya, T., Nakagawa, S., Koyama, T., Suenaga, K., and Uemura, D. (2002) Terpiodiene: a novel tricyclic alcohol from the Okinawan sponge Terpios hoshinota. *Chem Lett* **31**: 38–39.
Thacker, R.W., Diaz, M.C., Rützler, K., Erwin, P.M., Kimble, S.J., Pierce, M.J., and Dillard, S.L. (2007) Phylogenetic relationships among the filamentous

cyanobacterial symbionts of Caribbean sponges and a comparison of photosynthetic production between sponges hosting filamentous and unicellular cyanobacteria. *Porifera Res* **28**: 621–626.

Thacker, R.W., and Starnes, S. (2003) Host specificity of the symbiotic cyanobacterium Oscillatoria spongeliae in marine sponges, Dysidea spp. *Mar Biol* **142**: 643–648.

Thinesh, T., Jose, P.A., Hassan, S., Selvan, K.M., and Selvin, J. (2015) Intrusion of coral-killing sponge (Terpios hoshinota) on the reef of Palk Bay. *Curr Sci* **109**: 1030–1032.

Thinesh, T., Meenatchi, R., Pasiyappazham, R., Jose, P.A., Selvan, M., Kiran, G.S., and Selvin, J. (2017) Short-term in situ shading effectively mitigates linear progression of coral-killing sponge Terpios hoshinota. *PLoS One* **12**: e0182365.

Usher, K.M. (2008) The ecology and phylogeny of cyanobacterial symbionts in sponges. *Mar Ecol* **29**: 178–192.

Walker, B.J., Abeel, T., Shea, T., Priest, M., Abouelliel, A., Sakthikumar, S., *et al*. (2014) Pilon: an integrated tool for comprehensive microbial variant detection and genome assembly improvement. *PLoS One* **9**: e112963.

Wang, J.T., Chen, Y.Y., Meng, P.J., Sune, Y.H., Hsu, C.M., Wei, K.Y., and Chen, C.A. (2012b) Diverse interactions between corals and the coral-killing sponge, Terpios hoshinota (Suberitidae: Hadromerida). *Zool Stud* **51**: 150–159.

Wang, J.T., Hirose, E., Hsu, C.M., Chen, Y.Y., Meng, P.J., and Chen, C.A. (2012a) A coral-killing sponge, Terpios hoshinota, releases larvae harboring cyanobacterial symbionts: an implication of dispersal. *Zool Stud* **51**: 314–320.

Wang, J.T., Hsu, C.M., Kuo, C.Y., Meng, P.J., Kao, S.J., and Chen, C.A. (2015) Physiological outperformance at the morphologically-transformed edge of the Cyanobacteriosponge Terpios hoshinota (Suberitidae: Hadromerida) when confronting opponent corals. *PLos One* **10**: e0131509.

Webster, N.S., and Thomas, T. (2016) The sponge Hologenome. *mBio* **7**: e00135–e00116.

Whatley, J.M. (1977) The fine structure of Prochloron. *New Phytol* **79**: 309–313.

Wilkinson, C., and Fay, P. (1979) Nitrogen fixation in coral reef sponges with symbiotic cyanobacteria. *Nature* **279**: 527–529.

Wilkinson, C.R. (1983) Net primary productivity in coral reef sponges. *Science* **219**: 410–412.

Yilmaz, P., Parfrey, L.W., Yarza, P., Gerken, J., Pruesse, E., Quast, C., *et al*. (2014) The SILVA and "all-species living tree project (LTP)" taxonomic frameworks. *Nucleic Acids Res* **42**: D643–D648.

Yomogida, M., Mizuyama, M., Kubomura, T., and Reimer, J. D. (2017) Disappearance and return of an outbreak of the coral-killing cyanobacteriosponge Terpios hoshinota in southern Japan. *Zool Stud* **56**: 1–10.

Yu, C.H., Lu, C.K., Su, H.M., Chiang, T.Y., Hwang, C.C., Liu, T., and Chen, Y.M. (2015) Draft genome of Myxosarcina sp. strain GI1, a baeocytous cyanobacterium associated with the marine sponge Terpios hoshinota. *Stand Genomic Sci* **10**: 28.

Supporting Information

Additional Supporting Information may be found in the online version of this article at the publisher's web-site:

Fig. S1. Alpha diversity plots of each sample from different locations. (a) ASV richness estimated by Chao1. (b) Shannon's evenness index. (c) Faith's Phylogenetic Diversity box plot. Lines extending outside the boxes indicate variability outside the upper and lower quartiles. Points represent outliers.

Fig. S2. Taxonomic analyses of the *T. hoshinota* microbiome from different locations at the phylum (a) and genus (b) levels using 16S rRNA amplicon sequencing.

Fig. S3. Matrix of average amino acid identity between cyanobacteria that are closely related to the LD05 genome. The dendrogram was generated using the neighbour joining method.

Fig. S4. Complete phylogenetic tree of Fig. 5a. The tree includes 120 cyanobacteria from different genera. The branches with Ultrafast bootstrap (UFBoot) value >95% are highlighted with the red. The *Prochloron* genomes are labelled with yellow, and LD05 and SP5CPC1 are labelled with pink. *Vampirovibrio chlorellavorus* C was used as the outgroup.

Table S1. Summary of information on sampling.

Table S2. Proportions (%) of different cyanobacterial genera in *T. hoshinota*-associated cyanobacteria.

Table S3. Genomic features of LD05, *Prochloron*, and other phylogenetically-close cyanobacteria.

Table S4. Comparison of metabolic features in 'Paraprochloron' and *Prochloron*.